Available online at www.sciencedirect.com
SCIENCE DIRECT®
Journal of Chromatography A, 1053 (2004) 201–216
JOURNAL OF CHROMATOGRAPHY A
www.elsevier.com/locate/chroma

Influence of ignored and well-known zone distortions on the separation performance of proteins in capillary free zone electrophoresis with special reference to analysis in polyacrylamide-coated fused silica capillaries in various buffers☆
II. Experimental studies at acidic pH with on-line enrichment

Sheila Mohabbati[a], Stellan Hjertén[b], Douglas Westerlund[a,*]

[a] *Department of Analytical Pharmaceutical Chemistry, Uppsala University, Biomedical Center, P.O. Box 574, SE-75123 Uppsala, Sweden*
[b] *Department of Biochemistry, Uppsala University, Biomedical Center, P.O. Box 576, SE-75123 Uppsala, Sweden*

Abstract

The separation of acidic and basic model proteins was studied in capillary free zone electrophoresis in a polyacrylamide-coated, electroosmosis-free capillary at pH below their isoelectric points (p*I*) using various buffers at pH 2.7–4.8 with UV detection at 200 nm. The separation performance was significantly dependent on the coating quality, which may even differ within the same batch of capillaries. In addition, a washing step with 2 M HCl and the storage of the capillary in distilled water was essential for the performance. For high efficiency and resolution the choice of buffer constituents was extremely important which is discussed in quantitative terms in Part I. The most promising buffers were ammonium acetate and ammonium hydroxyacetate at pH 4 (ionic strengths: 0.12 and 0.15 M, respectively) with plate numbers up to 1 700 000 plates/m, corresponding to a zone width (2σ) of only 1 mm in a capillary with 40 cm effective length, when the injected samples were dissolved in a 10-fold diluted background electrolyte (BGE), a zone even narrower than those obtained in polyacrylamide gel electrophoresis, the characteristic feature of which is remarkably thin zones. In the experiment giving this plate number, the calculated variance for longitudinal diffusion was larger than all the other calculated variances (those for the width of the starting zone, Joule heating, sedimentation and the curvature of the capillary). Interestingly, the effect of capillary curvature was significant. In addition, the sum of all other imaginable variances (corresponding to various types of slow on/off kinetics and hyper-sharp peaks) was in the most successful experiments only 28–50% of the variance for longitudinal diffusion. One hundred- to two hundred-fold dilution of the BGE improved the detection limits and provided high precision in both migration times and peak areas with ammonium hydroxyacetate and ammonium acetate as background electrolytes. However, that high dilution increased the variance 140–400% for these buffers, respectively, at least partly due to conductivity or pH differences between the sample and buffer zones (hyper-sharp peaks). Sedimentation of the enriched sample, a factor that has not previously been treated theoretically or experimentally, was probably another reason for our finding that peak heights did not increase when the sample was dissolved in a buffer diluted more than 200-fold, although pH changes and in some cases thermal expansion in the capillary also may contribute. Loss of protein may occur at the ionic strength 0.01 and lower due to precipitation. Limits of detection were in the range 4–17 pmol of proteins with ammonium acetate as BGE. No indication of denaturation of proteins at pH 4 was observed. However, the separation performance at pH 3 was not satisfactory and loss of proteins was observed, possibly indicating such problems. The protein mobilities decreased unexpectedly from pH 4 to 3—a further indication of conformation changes.

Keywords: CZE; Proteins; Acidic buffers; Zone sharpening; Variance; Peak distortion; Joule heat; Sedimentation; Migration time; Conductivity and pH distortions; Hyper-sharp peaks; CLOD; Protein/buffer interaction

1. Introduction

Capillary electrophoresis is growing as one of the most powerful analytical techniques for the separation of proteins and peptides due to inherent advantages of the method, such

☆ For Part I, see Ref. [1].

* Corresponding author. Tel.: +46 18 4714287; fax: +46 18 4714392.
E-mail address: Douglas.Westerlund@farmkemi.uu.se (D. Westerlund).

0021-9673/$ – see front matter © 2004 Elsevier B.V. All rights reserved.
doi:10.1016/j.chroma.2004.08.071

as very high resolution, high separation efficiency, short analysis times, minimal sample volume requirement, and automated instrumentation [2–7]. Capillary electrophoresis of proteins has recently been reviewed [4–7]. An obstacle to such separations is the interaction of the negatively charged silanol groups on the capillary surface with positively charged proteins, leading to loss of efficiency, poor reproducibility in migration times, low protein recovery and decreased sensitivity [2,4]. However, hydrophobic interactions are also involved since negatively charged proteins exhibit similar drawbacks although to a smaller extent [4]. To overcome or suppress this protein adsorption, a variety of techniques have been developed. The simplest strategy consists of the use of electrolyte solutions at high pH values, considerably higher than the isoelectric point (p*I*) of the proteins to make both the proteins and the capillary wall negative, thus provoking strong electrostatic repulsion [2,8]. However, a simple increase in the pH of the background electrolyte (BGE) is often not sufficient to completely eliminate adsorption of proteins onto the capillary wall since hydrophobic and other interactions are not negligible (see above). This strategy has further the disadvantage of limiting the operational range of pH [2]. In addition, prolonged exposure to highly alkaline pH may denature proteins. Therefore, other methods to reduce the wall adsorption have expanded in popularity, including dynamic and static coating. Dynamic coating is performed by either adding neutral polymers to the BGE to shield the capillary wall [10,11], or suitable cations to decrease, neutralize or reverse the electroosmotic flow (EOF) [8,12]. Many of those additives may cause a decrease in detector signals, incompatibility with mass spectrometric detection and interactions with proteins [2]. However, the presence of polymers in the BGE may be an advantage in that they may increase the resolution by conferring a molecular-sieving structure on the separation medium [13]. In static wall coating, a hydrophilic neutral polymer is attached to the capillary wall, preferably followed by cross-linking [10]. The quality of the coating can be evaluated from EOF measurements and adsorption studies of basic proteins. Polyacrylamide is the most frequently used polymer for wall coating and the method was first developed by Hjertén [14] and later modified by Novotny and coworkers [15], Chiari et al. [16], Righetti and co-workers [17] and Blomberg and co-workers [18]. Other polymers, such as methyl cellulose [10,11], dextran [9], and polyvinyl alcohol (PVA) [19], have also been employed. Techniques based on isotachophoresis [20–24], isoelectric focusing [23–26], zone sharpening [27,28], the use of hollow fibers [29], and other techniques have been developed to enhance the sensitivity of protein detection. Sharp starting zones can be created if the electrical conductivity of the sample is lower than that of the buffer (BGE). This approach was introduced by Haglund and Tiselius [30] and was called zone sharpening. The required difference in conductivity (i.e. field strength) can also be achieved by displacement electrophoresis (or isotachophoresis as it was called later), as shown by Ornstein. He introduced the term "stacking" in analogy to the stacking of coins on top of each other [20]. These two enrichment methods often give the same degree of concentration [31], but should not be mixed up; "stacking" is based on displacement electrophoresis (isotachophoresis) and "zone sharpening" on zone electrophoresis. However, in the literature the term stacking is frequently used for zone sharpening techniques, the original and correct meaning of this term being ignored. A simple zone sharpening, an approach employed in this study, may increase the concentration of the proteins 1–3 orders of magnitude.

It is well known that proteins frequently denature upon prolonged exposure to low pH. Classical electrophoretic methods, such as moving boundary and paper electrophoresis, are therefore most often conducted at neutral and basic pH. This type of denaturation is time dependent. However, the much shorter analysis time in capillary free zone electrophoresis with attendant less zone broadening seems to make it possible to obtain reproducible electropherograms with high resolution in the pH range 4–5 [15,32]. The positive results obtained in our preliminary studies prompted us to study in detail the different mechanisms responsible for zone broadening effects. In order to minimize such effects we had to pay special attention to the choice of the coating and washing procedures to eliminate solute adsorption, the buffer constituents and their ionic strengths, the maximum degree of zone sharpening to avoid sedimentation of the starting zone, the width of the starting zone, different types of interactions with the proteins, and the suppression of solute interactions characterized by slow on/off kinetics, etc. The theoretical background to known and ignored zone broadening phenomena in capillary zone electrophoresis is treated in Part I of this series [1].

2. Experimental

2.1. Chemicals

All reagents were of analytical grade and all solutions were prepared in Nanopure water (Milli-Q water system, Millipore, Bedford, MA, USA). Albumin (bovine serum), carbonic anhydrase (bovine erythrocytes), α-chymotrypsinogen A (bovine pancreas), cytochrome *c* (horse heart), holotransferrin (human), lysozyme (chicken egg white), β-lactoglobulin (bovine milk), myoglobin (horse skeletal muscle) and ribonuclease A (bovine pancreas) were purchased from Sigma (St. Louis, MO, USA). The stock protein solutions were made in the concentration range 46–82 μM (1 mg/ml) in diluted running buffer. Buffers with ionic strengths 0.06–0.15 M were prepared from acetic acid (Riedel-de Haën, Germany), phosphoric acid (Merck, Darmstadt, Germany), formic acid (Kebo, Stockholm, Sweden), malonic acid and hydroxyacetic acid (Merck). *N*,*N*,*N*′,*N*′-Tetramethylethylenediamine (TEMED), ammonium persulfate and acrylamide (Bio-Rad, Hercules, CA, USA), and

γ-methacryloxypropyltrimethoxysilane (Sigma), were used to coat the fused silica capillaries.

The pH was adjusted to 2.72–4.00 by ammonia (Scharlau Chemie, Barcelona, Spain), sodium hydroxide (Merck) or triethanolamine (Riedel-de Haën). The Henderson–Hasselbalch equation ($pH = pK_a \log([A^-]/[HA])$) was used to calculate the concentration of the ionic component of the buffers. The final ionic strengths were calculated using equation: $\mu = 1/2 \sum c_i z_i^2$ and was used to characterize the buffers.

2.2. Apparatus

The CE experiments were performed, using an Agilent capillary electrophoresis system (Agilent Technologies, Waldbronn, Germany), interfaced to an HP Pentium II personal computer. Detection was accomplished on-capillary by recording UV absorbance at a short wavelength (200 nm) for high sensitivity.

Fused silica capillaries (50 μm i.d., 365 μm o.d.) were obtained from Polymicro Technologies (Phoenix, AZ, USA) and MicroQuartz (Munich, Germany). A 0.25-cm section of the polyimide coating was burned off by electrical heating for on-column detection [33]. The total lengths of the capillaries were 41.0–48.5 cm (8.5 cm after the detection window).

2.3. Polyacrylamide coating

The capillaries were coated with polyacrylamide to suppress electroosmosis and adsorption according to a modification of a procedure previously described [14]. In the pretreatment step the capillaries were washed with 1 M NaOH, 1 M HCl and finally water in order to obtain a fresh and clean inner capillary surface, which improves the homogeneity of the surface structure and thus the reproducibility of the coatings and consequently of the runs. Following drying with an air stream, the capillaries were filled with a 50% solution of γ-methacryloxypropyltrimethoxysilane in acetone, left for 20 h and then rinsed with acetone. The polymerization was carried out with 150 μl of acrylamide, 3 μl of ammonium persulfate and 3 μl of TEMED, all three components being 5% aqueous solutions (v/v for TEMED and w/v for the other two compounds). Non-covalently attached polymer was removed after 20 h simply by rinsing with water delivered by an HPLC pump. This procedure gave a thin, well-defined layer of the polymer covalently bound to the fused silica wall [14]. The quality of the coating was tested with acetone (10% aqueous solution) as a neutral electroosmotic marker, detected at 280 nm; the coating was considered efficient at an electroosmotic mobility less than 10^{-6} cm^2 V^{-1} s^{-1}.

2.4. Separation conditions

The electrophoretic runs were performed at 25 °C at a field strength between 300 and 500 V cm^{-1} with 10 s ramping. Prior to each experiment the capillaries were rinsed for 2 min with the running buffer, for 5 min with 2 M HCl (to eliminate possibly precipitated or adsorbed proteins, see Section 3.1) and then for an additional 2 min with the running buffer followed by a 60 s application of voltage for electrophoretic equilibration. The best reproducibility in migration time was achieved by replacing the used background electrolyte after each run with a fresh one (in experiments with ammonium acetate at pH 4 (ionic strength 0.12 M) the pH in the electrode vials changed 0.1–0.2 units by electrolysis during a run). The capillaries were stored overnight in water (hydrophobic interactions are small at low ionic strengths) after a 5 min wash with 2 M HCl, for release of possibly precipitated proteins. The samples were injected at the anodic end of the capillary, primarily electrophoretically at 8–1 kV for 2–16 s or, in a few cases, hydrodynamically at 50 mbar for 3–6 s. The proteins were dissolved in a 10–1000-fold diluted running buffer to a final concentration of 2.3–16.4 μM (0.05–0.2 mg/ml). Stock solutions were diluted down to 34–61 nM (0.00075 mg/ml) for studies on the concentration limits of detection, using enrichment of the sample by dissolving the protein in diluted running buffer.

3. Results and discussion

3.1. Capillary conditioning

Adsorption of one or more of the protein solutes may occur at non-coated spots on the capillary surface, which will generate a local electroosmotic flow [34]. The attendant zone broadening will be superimposed on other types of zone broadening. To prevent or at least minimize such distortions, the efficacy of different conditioning procedures was evaluated. Fig. 1 shows two electropherograms with lysozyme as analyte following two different washing procedures performed after previous runs. Thus, washing the capillary with 2 M HCl for 5 min followed by conditioning for 2 min with BGE seems to be efficient to release proteins accumulated at the capillary wall, probably in the form of precipitates (see below). It is in agreement with previous observations by Hjertén and Kubo [9], that PAA coatings withstand low pH values (0.1 M HCl). However, to our knowledge, the use of such a strong acid solution as that employed in this study has not previously been reported. Less strong acid solutions (0.5–1.0 M) were not adequately efficient. The accumulation of proteins at the capillary wall is probably caused by precipitation of proteins by the freely moving non-cross-linked polyacrylamide chains attached at a high ligand density to the capillary wall (free polymers are known to precipitate proteins), in analogy with the protein precipitates often observed at the bottom of the sample wells in slab gels of cross-linked polyacrylamide, following electrophoresis and staining (these precipitates are observed also when the protein sample has been freed from particulate material). In the bulk of the rigid polyacrylamide gels the polymer chains are cross-linked and no precipitates can be detected and the zones are very narrow

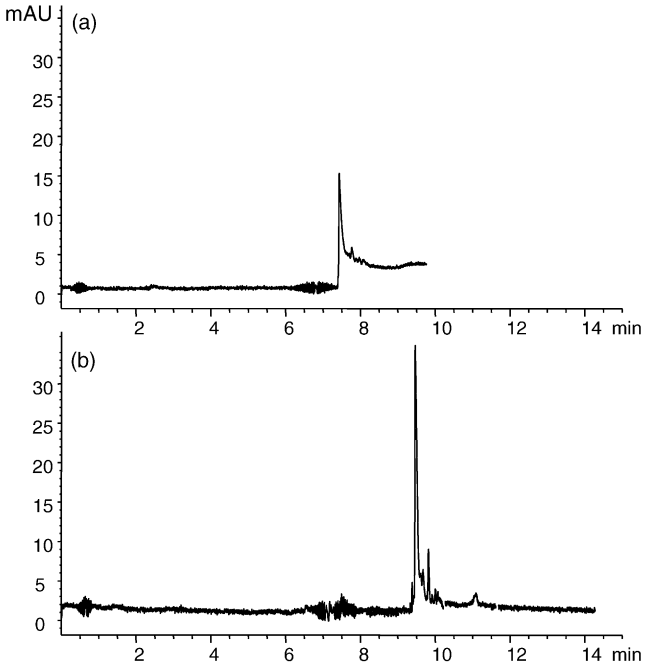

Fig. 1. The effect of capillary pre-conditioning with hydrochloric acid between runs. Analyte: lysozyme dissolved in 10 times diluted BGE to a final ionic strength of 14.2 μM (0.2 mg/ml). After each run the capillary was (a) rinsed with BGE for 2 min; and (b) rinsed with 2 M HCl for 5 min followed by a rinse with BGE for 2 min. BGE: 0.07 M ammonium acetate, pH 3.0. Voltage: 15 kV. Hydrodynamic sample application: 50 mbar for 6 s. Capillary length to the detector: 37.2 cm.

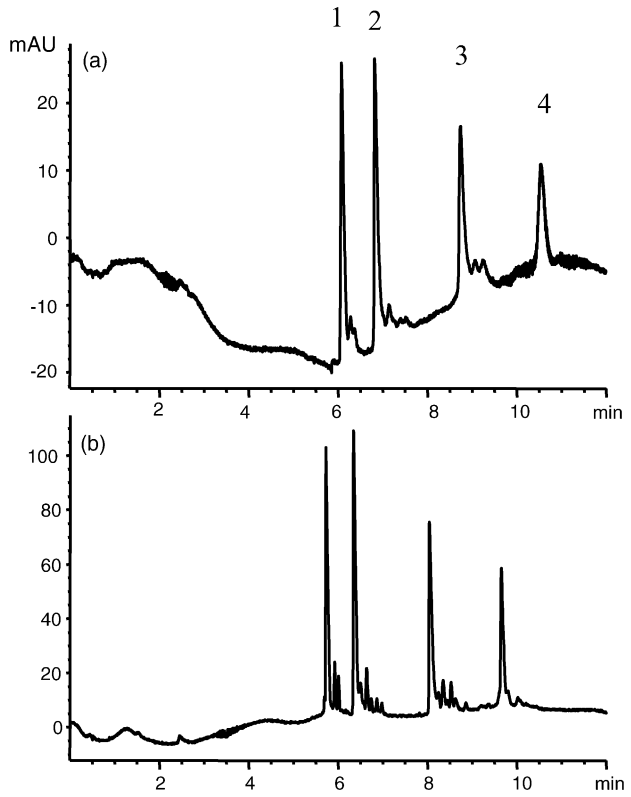

Fig. 2. The separation of four proteins in two different polyacrylamide-coated capillaries from the same batch and coated simultaneously. Proteins: (1) cytochrome *c*, (2) lysozyme, (3) ribonuclease A, and (4) α-chymotrypsinogen A. The proteins were dissolved in 100 times diluted BGE to the final concentrations of 4.6–8.2 μM (0.1 mg/ml). The coated capillaries were washed with 2 M HCl and then the BGE for 2 min. Separation conditions were the same for both runs: BGE: ammonium hydroxyacetate, pH 4.0 (ionic strength: 0.15 M). Voltage: 17.5 kV with 10 s ramping. Electrophoretic sample application: 2 kV for 8 s. Capillary length to the detector: 32.5 cm.

and symmetrical, indicating that proteins do not adsorb to the gel. Therefore, one cannot expect them to adsorb to the polymer chains in the wall coating, but rather to precipitate, as discussed above. The fact that the peaks obtained upon molecular-sieving of proteins in non-cross-linked polyacrylamide solutions are symmetrical indicates also that proteins do not adsorb to linear polyacrylamide chains [13,35,36]. The degree of enrichment of proteins at the capillary wall depends on the physico-chemical properties of the proteins (including their size) and the length and the concentration of the polyacrylamide chains. Accordingly, factors affecting these properties, including electrolyte species, ionic strength and pH, must be carefully considered in order to obtain a reproducible separation (these factors are of importance for the separation pattern also for other reasons). In a 2 M HCl solution the proteins are strongly positively charged and the silanol groups uncharged, i.e. the electrostatic attraction of the proteins to possibly non-coated surfaces of the capillary wall is completely eliminated. The varying properties of fused silica capillaries may also have a significant influence on the quality of the coatings [9]. It is further known that fused silica capillaries from different batches and even different sections within the same batch may have deviating surface structures [9]. Fig. 2 demonstrates a difference in the coating quality between two capillaries from the same batch, coated at the same time, using the same test protein mixture for the separation.

Six different buffers were studied in an attempt to gain insight into the effects of buffer character, ionic strength, and pH on the separation performance of some basic model proteins.

3.2. Buffers (background electrolytes)

3.2.1. Ammonium acetate

An initial pH of 3.0 was chosen for the BGE in order to make the proteins highly positively charged and thus minimize the run times (the p*I* values together with molecular masses, diffusion constants and radii are listed in Table 1). A disadvantage is the low buffering capacity of this solution (pK_a = 4.76) noticeable as an increasing current during the runs (an effect of electrolysis). However, the system gave highly consistent results in migration times. The electropherogram is presented in Fig. 3a. As the EOF is negligible, the observed migration of the cationic proteins towards the cathode is achieved entirely by electrophoresis. The effect of pH, i.e. the decrease in the net surface charge density of the proteins on the separation performance, was studied by

Table 1
Isoelectric points (p*I*), molecular masses, diffusion constants, and radius of the test proteins (at 25 °C)

Proteins	p*I*	M_r	D (cm^2 s^{-1})	r_p (Å)[a]
Cytochrome *c*	10.8	12 200	1.4×10^{-6}	14.1
Lysozyme	10.0	14 000	1.1×10^{-6}	14.8
Ribonuclease A	8.7	13 500	1.1×10^{-6}	14.6
α-Chymotrypsinogen A	8.8	21 600	0.9×10^{-6}	17.1
β-Lactoglobulin	5.2	37 000		20.4
Carbonic anhydrase	8.0	25 000		17.9
Holo-transferrin	6.0	79 000		26.3
Albumin	4.5	68 000		25.0
Myoglobin	>8.0	16 000		15.4

[a] Calculated from the approximate equation in Section 2.10.2 in Part I [1].

running the proteins at higher pH values. At pH 3 the positive net charge of the proteins should be equal to or larger compared to the charge at pH 4 and, thus, the protein should migrate faster. Observe, however, that a pH as low as 3 may cause protein denaturation (see Sections 3.3, 3.5, and 3.6). An indication of conformation changes is the unexpected decrease of migration times at pH 3 compared to pH 4. Since at pH 3 the concentration of uncharged acetic acid is higher and possible

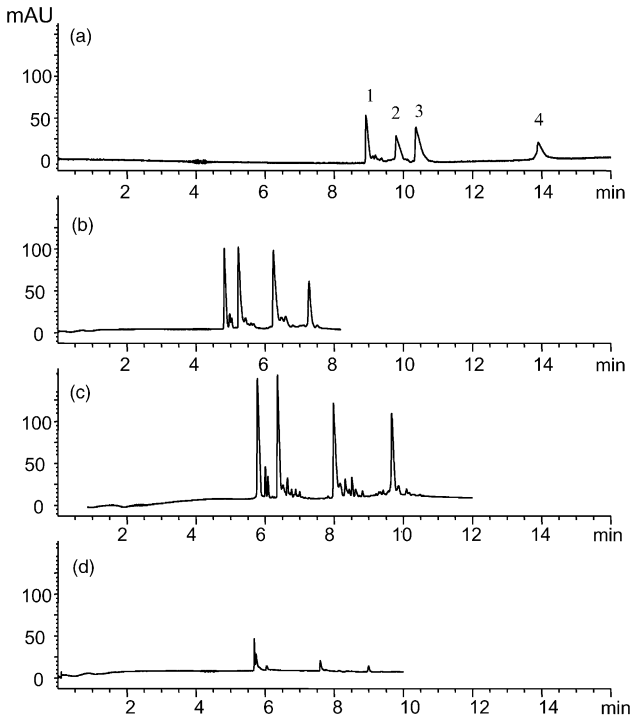

Fig. 3. The influence of varying compositions and pH of ammonium acetate buffers on the separation of four standard basic proteins. BGE: ammonium acetate. Ionic strengths and pH: (a) 0.07 M, pH 3.0; (b) 0.07 M, pH 4.0; (c) 0.12 M, pH 4.0 (for a magnified version see Fig. 5b); and (d) 0.12 M, pH 4.76. Proteins: (1) cytochrome *c*, (2) lysozyme, (3) ribonuclease A, and (4) α-chymotrypsinogen A. All proteins were dissolved in 100 times diluted BGE to the final concentrations of 4.6–8.2 μM (0.1 mg/ml). The capillary was pretreated prior to each run as described in the legend to Fig. 1. Voltage: 17.5 kV with 10 s ramping. Electrophoretic sample application: 1 kV for 16 s. Capillary length to the detector: 40 cm.

interaction between this buffer constituent and the proteins may, as an alternative, explain the lower migration velocities, the asymmetry of the peaks, as well as changes in the relative migration velocities. It is known that the non-charged form of acetic acid forms a complex with proteins [37], which is in agreement with the observation that the cytochrome *c* peak in Fig. 3a is (close to) hyper-sharp, whereas the peak in Fig. 3b is not.

A strong improvement of efficiency was obtained at pH 4 compared to pH 3 (compare Fig. 3a and b). The separation of small impurity/isomer peaks also improved significantly at pH 4. Upon an increase in ionic strength of the BGE the mobilities of proteins decrease which explains the longer migration times in Fig. 3c compared to those in Fig. 3b (Eq. (19) in Part I [1]). The increase of the ionic strength from 0.07 to 0.12 M at pH 4.0 (Fig. 3b and c) had a positive impact on peak efficiency (50–100%) and resolution (more isomers/impurities resolved, see Fig. 5b for details). Upon an increase in ionic strength of the buffer, the difference in mobilities of the buffer ions and the proteins increases (Eq. (19) in Part I [1]), i.e. $\Delta\kappa$ (Eq. (8)) increases and consequently the asymmetry of the peaks should increase. Because of the higher buffering capacity of the more concentrated buffer ΔpH is smaller which further increases the asymmetry since the distortions caused by $\Delta\kappa$ and ΔpH counteract each other (see Section 2.7 in Part I [1]). However, as mentioned above, the resolution for isomers/impurities increased at pH 4; several more peaks are visible in Fig. 3c compared to Fig. 3b. The seemingly broader and more asymmetric peaks in Fig. 3b are then probably due to co-migration of the main peaks with isomers/impurities.

The ratios between the migration times of cytochrome *c*, lysozyme, ribonuclease A and α-chymotrypsinogen at the ionic strength 0.12 M (Fig. 3c) and 0.07 M (Fig. 3b) were 1.19, 1.21, 1.26, and 1.33. The ratios between the calculated inversed values of the mobilities of these proteins were estimated at 1.17, 1.18, 1.17, and 1.18 ($t \propto 1/u = (1/u_0)(1 + (\sqrt{\mu}/3)r_p)$; see Eq. (19) in Part I [1]). The protein radius r_p was calculated as described in Section 2.10.2.2. in Part I [1] (see also Table 1). The agreements between the experimental and calculated values are surprisingly good, considering the very approximate, calculated values of the protein radii (Table 1).

Furthermore, the variance of adsorption (Eq. (6) in Part I [1]) should increase at increasing field strength. Experiments show (Fig. 4) that the trend is opposite. Obviously adsorption effects are negligible.

At pH 4.76, equal to pK_a of acetic acid, a radical impairment of the separation was observed (Fig. 3d) as well as a dramatic decrease of the UV response. The migration pattern is different; an explanation could be complex formation between the protein and the acetate ion, which has several-fold higher concentration at pH 4.76 compared to pH 4 (see Sections 3.9 and Ref. [3] in Part I [1]). A complex may also shift the UV spectrum explaining the decrease in signal. The results displayed in Fig. 3 illustrate the importance of

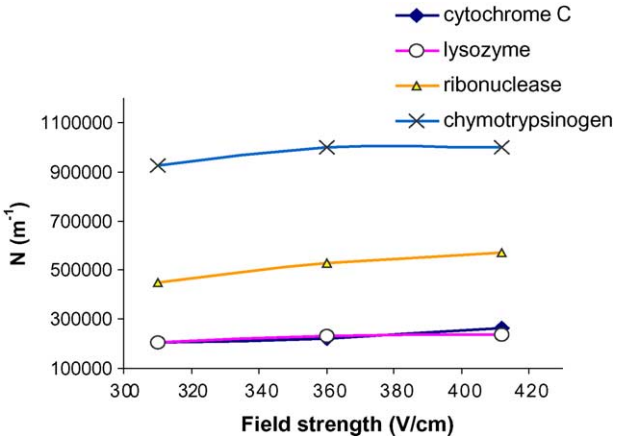

Fig. 4. A plot of efficiency (*N*) against field strength, BGE: ammonium acetate, pH 4.0 (ionic strength 0.12 M).

selecting suitable pH and ionic strength in protein separations and protein purity studies; the effects can be rather dramatic.

Based on these studies, 120 mM ammonium acetate, pH 4.0 was considered as the most suitable buffer (see Fig. 5). The migration times (Table 2), peak areas and peak widths at half the height (Table 3) were highly repeatable. Observe that the proteins were injected in BGE diluted 100 times (see Section 3.8 for a general discussion on zone sharpening). The studied proteins are basic and will be positively charged in an acidic buffer, and since the number of theoretical plates, at least in theory, under certain conditions, is directly proportional to the number of charges, it is in general more favorable to use acidic conditions to attain efficient separations. One may expect the pH 4.0 buffers to be appropriate also for acidic proteins, i.e. those with p*I* values 5–7, because they are positively charged at this pH.

3.2.2. Ammonium formate

Ammonium formate is like ammonium acetate compatible with MS detection and is, therefore, of great interest for protein identification studies. It was used at pH 2.7 where the buffer capacity is relatively low (pK_a = 3.75). Separation of both basic and acidic proteins is illustrated in Fig. 6. However,

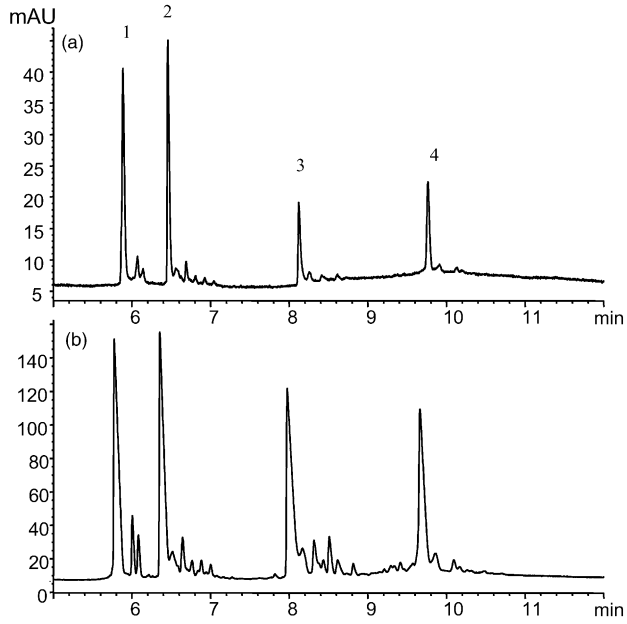

Fig. 5. Separation of four proteins in ammonium acetate, pH 4 (ionic strength 0.12 M). The proteins (1) cytochrome *c*, (2) lysozyme, (3) ribonuclease A, and (4) α-chymotrypsinogen A, were introduced in (a) 10 and (b) 100 times diluted BGE to the final concentrations of 4.6–8.2 μM (0.1 mg/ml). Separation conditions: Voltage: 17.5 kV with 10 s ramping. Electrophoretic sample application: 1 kV for 16 s. Capillary length to the detector: 40 cm.

when stored in this solution, some of the proteins seemed to degrade with time; a few peaks (e.g. the cytochrome *c* peak) even disappeared completely at consecutive runs. These observations probably reflect the increased risk of denaturation of proteins at this low pH (see Sections 3.3, 3.5, and 3.6).

3.2.3. Ammonium hydroxyacetate

High efficiency and resolution and excellent isomer/impurity separations were accomplished with this buffer (Fig. 7), which had the ionic strength 0.15 M and pH 4.0. The repeatabilities for run-to-run migration time, peak area and peak width were good, only slightly lower than with ammonium acetate (Tables 2 and 3), indicating no or negligible denaturation or loss of protein. The two-fold higher dilution of the hydroxyacetate buffer for the sample application

Table 2
Migration time repeatabilities (R.S.D. %, n = 10)

	Ammonium acetate, pH 4.0 (Fig. 5b)[†a]	Ammonium hydroxyacetate, pH 4.0 (Fig. 7b)[‡a]	Triethanolamine- hydroxyacetate, pH 4.0 (Fig. 9)[†b]
Buffering capacity	0.036	0.35	0.58
Ionic strength (M)	0.12	0.15	0.25
Proteins			
Cytochrome *c*	0.70	1.26	3.65
Lysozyme	0.55	1.13	3.78
Ribonuclease A	0.75	1.20	4.61
α-Chymotrypsinogen A	0.93	0.92	5.54

Samples in BGE diluted [†]100 and [‡]200 times.
[a] Injection: 1 kV/16 s.
[b] Injection: 8 kV/2 s.

Table 3
Peak area and peak width (at half height) repeatabilities for four basic proteins in two high-resolution running buffers[a] (R.S.D. %, n = 10)

	Ammonium acetate, pH 4.0 (Fig. 5b)[†]		Ammonium hydroxyacetate, pH 4.0 (Fig. 7b)[‡]	
	Peak area	Peak width	Peak area	Peak width
Ionic strength (M)	0.12		0.15	
Proteins				
Cytochrome *c*	2.2	2.7	4.5	8.2
Lysozyme	1.9	1.8	2.4	2.5
Ribonuclease A	1.8	1.5	1.5	1.8
α-Chymotrypsinogen A	1.1	1.6	1.4	1.7

[a] Samples in BGE diluted [†]100 and [‡]200 times. Injection: 1 kV/16 s.

(samples dissolved in 200-fold diluted BGE compared to 100-fold in ammonium acetate experiments) gives a sedimentation rate and distance, which are two-fold higher (Eqs. (5) and (6)) that may explain the somewhat lower reproducibility of peak area and peak width (Section 3.7).

3.2.4. Triethanolamine-malonate and triethanolamine-hydroxyacetate

Triethanolamine has been demonstrated to be an efficient capillary wall adsorption inhibitor [38–40]. It has a high affinity for charged silanol groups providing at adequate concentrations a reversed electroosmotic flow in uncoated fused silica capillaries. A drawback is that the compound or impurities have a relatively high UV absorbance at 200 nm. A separation of five basic and acidic proteins with triethanolamine-malonate, pH 3, as BGE is shown in Fig. 8 (malonic acid has pK_{a1} = 2.75), illustrating an inadequate separation of isomer/impurity peaks. The signal intensity of all proteins decreased continuously at successive runs again demonstrating the unsuitability of using such a low pH as 3 for the test proteins.

With triethanolamine-hydroxyacetate, pH 4 (pK_a of hydroxyacetic acid is 3.83) high efficiencies (up to 1 000 000 N/m) and good resolution of the isomer/impurity peaks were obtained when the sample (in 100-fold diluted BGE) consisted of basic proteins (the top four in Table 1) (Fig. 9). However, less good repeatabilities in migration times (Table 2), compared to the repeatabilities of ammonium acetate and hydroxyacetate buffers were obtained; the reason might be the different injection conditions (higher voltage and shorter injection times) used with this buffer, and a possible variation in current caused by bubbles and/or precipitates (see Section 2.10.3 in Part I [1]).

3.2.5. Phosphate

For phosphate buffers, pH 3, the separation profile was strongly dependent on their ionic strengths, as illustrated in Fig. 10 (observe the shorter capillary length in Fig. 10c). More peaks appear at higher ionic strengths. The low ionic strengths in (a) and (b) may have caused precipitation of some of the proteins and thus explain the absence of some of the peaks in

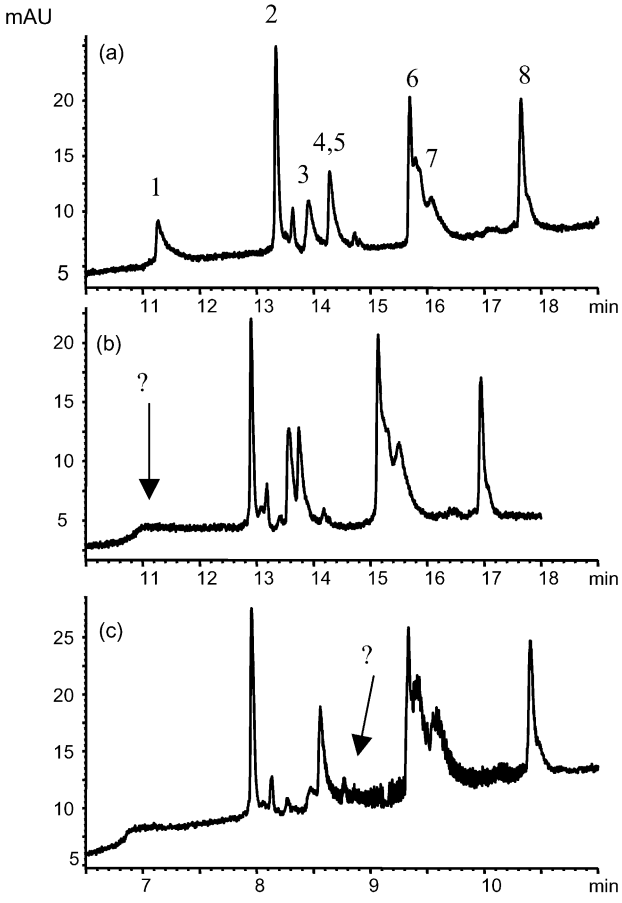

Fig. 6. Electropherograms illustrating instability of basic and acidic proteins in successive runs in the BGE 0.068 M ammonium formate, pH 2.7. (a) 1st run, (b) 3rd run, and (c) 4th run (the injected samples were taken from the same vial). Separation conditions: voltage: 10 kV in (a) and (b) and 15 kV in (c) with 10 s ramping in all three runs; electrophoretic sample application: 8 kV for 2 s. Capillary length to the detector 37.2 cm. Proteins: (1) cytochrome *c*, (2) lysozyme, (3) myoglobin, (4) ribonuclease A, (5) β-lactoglobulin, (6) holo-transferrin, (7) carbonic anhydrase, and (8) α-chymotrypsinogen A. The solutes were dissolved in 10 times diluted BGE to the final concentrations 2.7–4.8 μM (0.06 mg/ml).

the electropherogram 10a and the reduction in their heights in electropherogram 10b. The electropherograms were recorded up to 20 min without the appearance of additional peaks. It is not likely that these variations in the appearance of the electropherograms are caused by adsorption of the proteins onto the capillary wall (Part I [1]), because (1) the peaks in electropherogram 10a do not exhibit more tailing—rather less—than those in electropherograms 10b and 10c and (2) the relative migration velocities are roughly the same in all these electropherograms: upon adsorption, different proteins interact differently with the capillary wall (Eq. (6) in Part I [1]), which affects the migration velocities differently. Observe that tailing is a necessary, but not sufficient condition for adsorption.

Poor resolution with few visible isomer/impurity peaks and irreproducible migration times even at the highest ionic

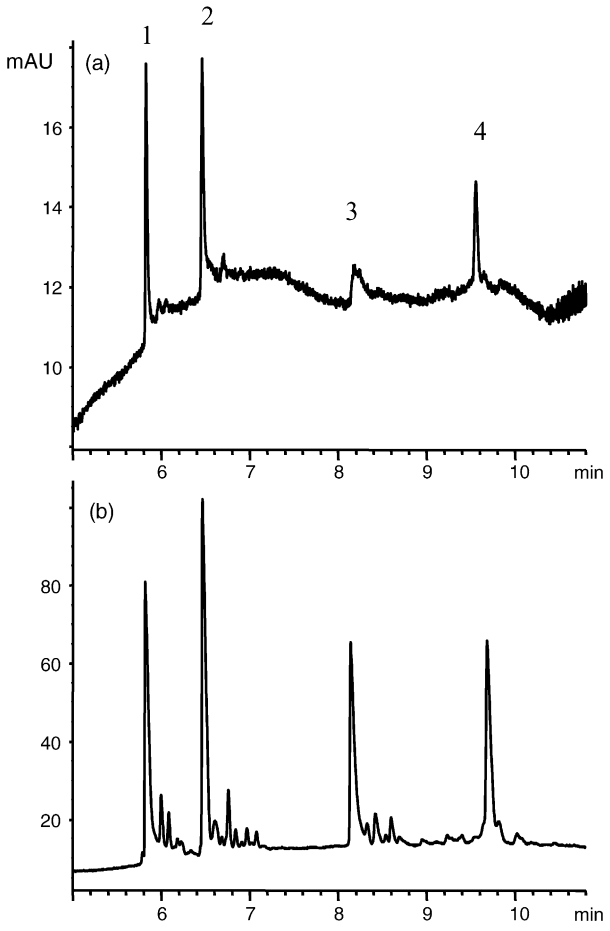

Fig. 7. Separation of four proteins using optimized buffer condition: ammonium hydroxyacetate, pH 4.0 (ionic strength: 0.15 M). The proteins (1) cytochrome *c*, (2) lysozyme, (3) ribonuclease A (the peak is relatively small in experiment (a) for unknown reasons), and (4) α-chymotrypsinogen A, were introduced in (a) 10 times and (b) 200 times diluted BGE to the final concentrations 4.6–8.2 μM (0.1 mg/ml). Voltage: 17.5 kV with 10 s ramping. Electrophoretic sample application: 1 kV for 16 s. Capillary length to the detector: 40 cm.

strength were the main drawbacks of this buffer system. Furthermore, of the seven proteins introduced only three to five peaks were observed. The results add to our experience that a pH as low as 3 seems to be unsuitable for the separation of studied proteins, irrespective of buffer components (acetate, formate, malonate, and phosphate).

3.3. The background electrolytes and some relevant physical data

The generation of Joule heat in different buffers was studied by plotting the current against the voltage (Table 4) The critical field strength, according to our definition, is the field strength corresponding to a 10% increase of the current relatively the extrapolated linear relationship between current and voltage. The effect of buffer concentration on the critical field strength is reflected in the data for the phosphate buffer. The influence of the size of the buffer components on the

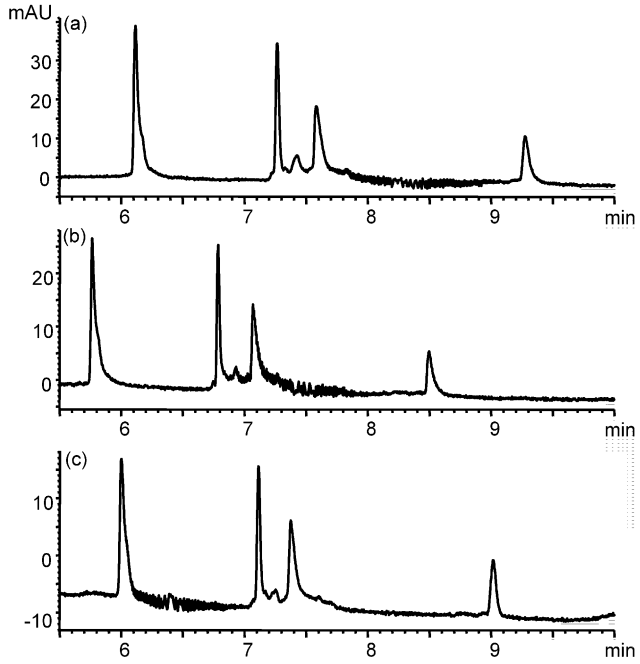

Fig. 8. Electropherograms illustrating instability of the proteins in *successive* runs in the BGE 0.1 M triethanolamine-malonate, pH 3.0. Notice the decrease in peak intensities and the variation in migration times. Proteins: cytochrome *c*, lysozyme, myoglobin, β-lactoglobulin and α-chymotrypsinogen A: All proteins were dissolved in 10 times diluted BGE to the final concentrations 4.6–8.2 μM (0.1 mg/ml). Voltage: 15 kV with 10 s ramping. Electrophoretic sample application: 2 kV for 8 s. Capillary length to the detector: 32.5 cm.

conductivity is illustrated by the differences in the limiting voltage between ammonium and triethanolamine hydroxyacetate buffers, respectively. In spite of a much higher ionic strength, 0.25 M compared to 0.15 M, the limiting voltage is higher for the triethanolamine-based buffer, because the

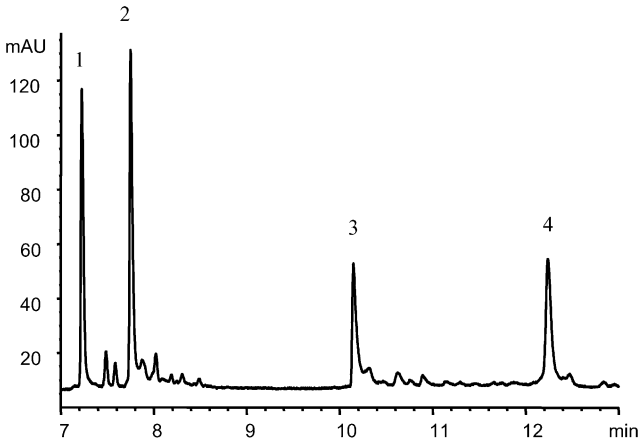

Fig. 9. Separation of four proteins using 0.25 M triethanolamine-hydroxyacetate, pH 4.0, as BGE. Proteins: (1) cytochrome *c*, (2) lysozyme, (3) ribonuclease A, and (4) α-chymotrypsinogen A, all dissolved in 100 times diluted BGE to the final concentrations 4.6–8.2 μM (0.1 mg/ml). Voltage: 15 kV with 10 s ramping. Electrophoretic sample application: 2 kV for 8 s. Capillary length to the detector: 32.5 cm.

Table 4
Development of Joule heat in the buffers studied

Buffer	pK_a (acid)	pH	Ionic strength (M)	Critical field strength (V cm^{-1})	Buffering capacity (M/ΔpH)
Ammonium formate	3.75	2.7	0.068	288	0.005
Ammonium acetate	4.76	4.0	0.12	247	0.036
Ammonium acetate	4.76	4.8	0.12	329	0.29
Ammonium hydroxyacetate	3.78	4.0	0.15	268	0.35
Triethanolamine-malonate	2.85	3.0	0.10	371	0.23
Triethanolamine-hydroxyacetate	3.78	4.0	0.25	288	0.58
Phosphate buffer	2.15	3.0	0.06	412	0.023
Phosphate buffer	2.15	3.0	0.08	329	0.029
Phosphate buffer	2.15	3.0	0.1	247	0.046

larger buffer ions have lower mobilities and, thus, give lower $\Delta\kappa$ values (Eq. (8)) and often less asymmetry.

3.4. Zone sharpening studies

The conductivity of the sample (phase I) is considerably lower than that of the running buffer (phase II) (Fig. 8a in Part I [1]). The enrichment factor, ef, defined as the ratio between the protein concentration in phase II and I, following the enrichment can in a very approximate form be written:

$$\text{ef} \approx \frac{\kappa^{\text{II}}}{\kappa^{\text{I}}} \tag{1}$$

where κ^{I} and κ^{II} are the conductivities of the sample and buffer solutions, respectively (Eq. (21) in Part I [1]) The enrichment factor is obviously inversely proportional to the conductivity of the diluted buffer, in other words approximately directly proportional to the dilution of the buffer.

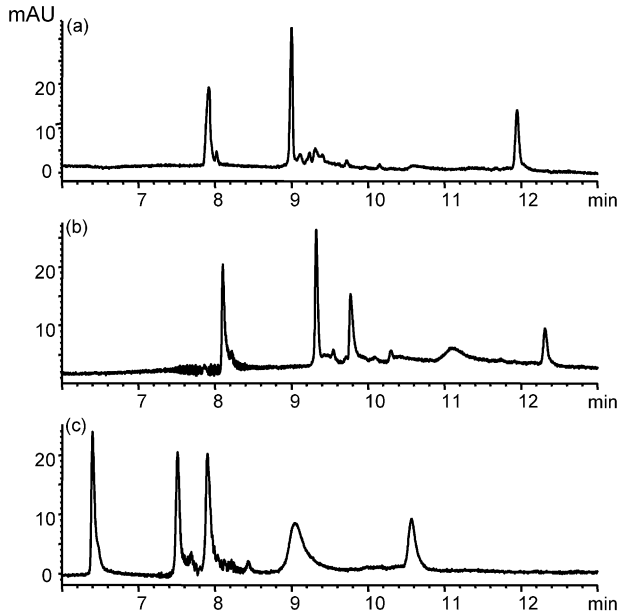

Fig. 10. Separation of seven proteins at different ionic strengths of the BGE, sodium phosphate buffer, pH 3.0 (pK_a = 2.1). Ionic strengths: (a) 0.06 M, (b) 0.08 M, and (c) 0.1 M. Voltage: 15 kV with 10 s ramping. Electrophoretic sample application: 8 kV for 2 s. Proteins: cytochrome *c*, lysozyme, myoglobin, β-lactoglobulin, holo-transferrin, carbonic anhydrase, and α-chymotrypsinogen A. All proteins were dissolved in 10 times diluted BGE to the final concentrations 4.6–8.2 μM (0.1 mg/ml). Capillary length to the detector: (a) and (b) 37.2 cm, (c) *only* 32.5 cm.

The proteins were generally introduced by electrophoretic injection following their dissolution in diluted BGE at a concentration of 4.6–8.2 μM (0.1 mg/ml). The higher electrophoretic migration velocity of the proteins in the low-conductivity BGE zone gives rise to an enrichment of proteins at the *virtually stationary* boundary between high and low BGE concentration (see Section 3.7 in Part I [1]). To evaluate the effect of the magnitude of this conductivity difference on the zone sharpening, the proteins were dissolved in 10–1000-fold diluted high-resolving BGE: ammonium acetate and ammonium hydroxyacetate, both at pH 4, with the ionic strengths 0.12 and 0.15 M, respectively (Fig. 11; the same absorbance scale is used for all 10 electropherograms to facilitate comparisons of the zone sharpening effects). The intensity of the peaks was enhanced 10–30 times, when the dilution factor increased from 10 to 1000, i.e. the enrichment effect was lower than that predicted by Eq. (1). The repeatabilities of both peak areas and peak heights at 100- and 200-fold dilutions for ammonium acetate and ammonium hydroxyacetate buffers, respectively, were high (Table 3), demonstrating a high potential of the method for quantitative determinations. However, the results were not reproducible at the highest dilution factors, 500–1000 times, and there was no or only a small increase in peak heights or even a small decrease when the dilution factor exceeded 200 (Fig. 11d and e). This is probably due to sedimentation and pH effects (see Sections 3.7 and 3.8) and possibly thermal expansion effects (see Part I [1], Sections 2.10.1.1 and 2.10.1.3).

3.5. Migration times

A logarithmic derivation of Eq. (29) in Part I [1] gives:

$$\frac{\Delta t}{t} = \frac{\Delta|\Delta X_0(\kappa^{\text{II}}/\kappa^{\text{I}}) + L_t|}{|\Delta X_0(\kappa^{\text{II}}/\kappa^{\text{I}}) + L_t|} + \frac{|\Delta u_{\text{p}}^{\text{II}}|}{|u_{\text{p}}^{\text{II}}|} \tag{2}$$

Even if $\Delta X_0 < 1$ mm, $\Delta X_0(\kappa^{\text{II}}/\kappa^{\text{I}})$ can adopt large values at large dilutions of the buffer and is in such runs not negligible in comparison with L_t. One can expect the ΔX_0-value to vary in a series of experiments since they are extremely small and, therefore, also $(\Delta X_0(\kappa^{\text{II}}/\kappa^{\text{I}}) + L_t)$. Accordingly,

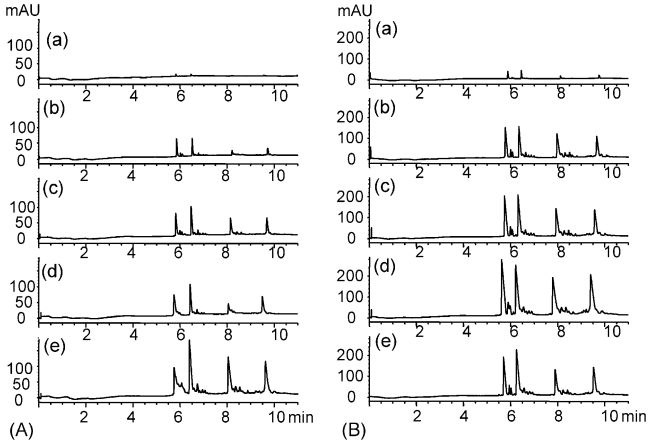

Fig. 11. Zone sharpening effects on peak intensities. The proteins (1) cytochrome *c*, (2) lysozyme, (3) ribonuclease A, and (4) α-chymotrypsinogen A were added to the BGE (A) ammonium hydroxyacetate, pH 4.0 (ionic strength: 0.15 M) and (B) ammonium acetate, pH 4.0 (ionic strength 0.12 M), diluted (a) 10 times, (b) 100 times, (c) 200 times, (d) 500 times, and (e) 1000 times. Voltage: 17.5 kV with 10 s ramping. Electrophoretic sample application: 1 kV for 16 s. Capillary length to the detector: 40 cm. Protein concentration: the same in all runs (4.6–8.2 μM: 0.1 mg/ml). Observe that the scales for peak intensities in A and B differ.

the migration times may vary considerably from run to run in a series of experiments with electrophoretic zone sharpening and more the higher the dilution of the buffer. These inevitable variations in migration times appear, of course, also when the migration time is calculated from the common relation $t = L_d/uE$. In accordance with the above discussions the largest variations in migration time was obtained for the experiment with the highest dilution factor (Table 2). In addition, a low buffering capacity of the separation medium (phase II) may cause a change in its pH and, therefore, in its conductivity during the course of a run, for instance by electrolysis in the electrode vessels and/or uptake of carbon dioxide from air and, consequently, in the mobilities of the proteins (the second term). Nor are these alterations of relevant parameters reproducible, which contribute to the difficulty to obtain repeatable migration times in experiments where very strong zone sharpening is employed ($\kappa^{II}/\kappa^{I} > 100$–200).

3.6. Effect of Joule heat on the diffusion constants

The temperature rise within the capillary was estimated from plots of the current against field strength (Fig. 3 in Part I [1]), using Eq. (4) in Ref. [40] and Eq. (71a) in Ref [21]:

$$\Delta T = \frac{I(\overline{T}_2) - I(\overline{T}_1)}{0.027 I(T_1)} \tag{3}$$

where $\overline{T}_1$ and $\overline{T}_2$ are the average values of the temperatures at the start and at steady state, respectively, $I(\overline{T}_2)$ is the current at temperature $\overline{T}_2$, i.e. at a certain field strength, $I(\overline{T}_1)$ is the current at the lower temperature $\overline{T}_1$, corresponding to the extrapolated straight line in the above plot, the coefficient 0.027 is the increase in conductivity per degree. Using Eq. (3), the average temperature rise in the buffer was estimated at 10 and 7 °C in the electrophoresis experiments in ammonium acetate (ionic strength 0.12 M) and ammonium hydroxyacetate (ionic strength 0.15 M), respectively, both at pH 4 (Figs. 5 and 7).

The diffusion coefficients in Table 1 refer to 25 °C. They were recalculated for the actual temperature by Eq. (4) [41]:

$$D_{T_2} = \frac{T_2}{T_1}\frac{\eta(T_1)}{\eta(T_2)} D_{T_1} \tag{4}$$

and used to calculate the variances for diffusion, Joule heating, and sedimentation (Eqs. (2), (5), and (13) in Part I [1]).

3.7. Zone broadening caused by sedimentation

A possible explanation for protein losses and irreproducible results at high sample dilution degrees is sedimentation of the concentrated protein zone in the enrichment step and at the start of the run, as is described in detail in Part I [1]. The concentrated protein sample is confined in a thin layer (see Section 3.7 in Part I [1]) close to the inlet of the vertical section of the capillary with a much higher density than that of the protein solution below the boundary (and that of the buffer in the electrode vessel). Part of the protein solution will, therefore, sediment and leave the capillary in its vertical section and an additional part of the sample will be washed away when the sample is replaced by the buffer vial (see Fig. 4b in Part I [1]).

The maximum sedimentation velocity and sedimentation distance at the center of the capillary, including the effect of radial diffusion, are determined by Eqs. (5) and (6), respectively (Part I [1]):

$$v_{\max\ D} = \frac{R^3 g}{8\eta\sqrt{2Dt}}(\rho_s - \rho_b) \tag{5}$$

$$d_{\max\ D} = \frac{R^3 g\sqrt{t}}{4\eta\sqrt{2D}}(\rho_s - \rho_b) \tag{6}$$

where g is the gravitational acceleration (≈980 dyne cm^2), R the radius of the capillary (0.0025 cm in our experiments), ρ_s and ρ_b the densities of the sample and buffer solutions, respectively [$\rho_s - \rho_b$ = 0.003 (g cm^{-3}) for a 1% aqueous protein solution], and η the viscosity [≈0.0077 P cm^{-1} s^{-1} for the electrophoretic experiments in ammonium hydroxyacetate at 32 °C and 0.0076 P cm^{-1} s^{-1} in ammonium acetate at 35 °C, respectively (see Section 3.6)]. The density difference can be calculated from the relation [42]:

$$\rho_s - \rho_b = c(1 - \bar{v}_p\rho_b) \quad (7)$$

where c is the concentration of the solute, and $\bar{v}$ the partial specific volume of the solute (for proteins often 0.73 cm^3 g^{-1}). Calculations applying Eqs. (5) and (6) show that at a dilution degree of 100 times (we assume that the protein concentration has increased 100-fold), the sedimentation velocity is 0.003 mm/s and the sedimentation distance is 0.17 mm (for t = 30 s) (see Section 2.10.1 in Part I [1]), which is significant since the enriched sample zone is located very close to the tip of the capillary (see Section 3.7 in Part I [1]) and the experimentally determined length of the starting zone is only 0.04–0.4 mm, as a plot of plate height against the reciprocal of the field strength indicated (details of the calculations are given in Part I [1]). This loss of protein is reinforced by the subsequent washing procedure (Fig. 8b in [1]) and perhaps by pH changes and an attendant decrease in protein mobilities (see Section 2.10.1.5 in [1]). In other words, one cannot expect the enrichment factor to become as high as predicted by Eq. (1), particularly not at high dilution degrees (i.e. at high protein concentrations at the interface), which cause the sedimentation and the pH change to become more pronounced. Therefore, it is not surprising that a dilution of the BGE more than 200-fold did not increase the peak intensities.

The ratios between the areas of the peaks for a particular protein in the electropherograms, i.e. the ratio of the amounts of this protein (Fig. 11a–d) are in agreement with this conclusion, since their ratios increase at a rate much less than the dilution of the buffer (Eq. (1)). Interestingly, in Fig. 11B(e) (BGE: ammonium acetate) the peak areas are smaller than those in Fig. 11B(d), although they should be two-fold larger according to Eq. (1). A likely explanation is that the enrichment of the proteins at the concentration boundary is highest in the experiments shown in Fig. 11A(e) and, thereby, the sedimentation velocity (Eq. (5)) and possible pH changes. To conclude, the reproducibility upon the enrichment of the protein sample may be low, because: (i) the sedimentation distance ($d_{\max D}$) and possible pH changes are both concentration and time dependent and (ii) upon contact with the BGE following the enrichment the amount of proteins washed out is probably not the same in a series of experiments. Accordingly, a final dilution factor of 200 for the ammonium hydroxyacetate system and 100 for the ammonium acetate system were chosen as the most advantageous regarding sensitivity enhancement and reproducibility in zone sharpening, migration times, peak widths, and peak areas (Figs. 10B(b) and 11A(c) and Tables 2 and 3).

The efficiencies were impaired by the high dilution degrees (Table 5): the number of plates decreased four to six-fold for the ammonium acetate buffer when the sample dilution degree was increased from 10 to 100 (Fig. 5). The decrease in plate number upon an increase of the dilution from 1/10 to 1/200 for the ammonium hydroxyacetate buffer was smaller, 1.5–2.6 times.

The higher buffering capacity of this buffer and attendant less increasing pH (caused by uptake of carbon dioxide from the air and electrolysis at the cathode) yield a less decrease in the mobility of the proteins and, therefore, higher protein concentrations in the starting zone, which may explain the higher peak intensities in Fig. 11B compared to those in Fig. 11A.

3.8. Zone distortions caused by conductivity and pH differences

The conductivity difference is determined by the expression [1,43,44]:

$$\Delta\kappa = \frac{c_P}{u_P}(u_A - u_P)(u_R - u_P) \quad (8)$$

where $\Delta\kappa$ is the difference in conductivity between sample zone and surrounding BGE zones; c_P the concentration of a protein in the solute zone (C/ml); u_A, u_P, and u_R are the mobilities of the co-ion (the buffer ion having the same sign

Table 5
Efficiencies (number of theoretical plates per meter), calculated using statistical moments for basic test proteins separated in a polyacrylamide coated capillary at different buffer conditions. Ionic strengths: (1): 0.12 M, (2): 0.15 M

Sample dilution	Ammonium acetate, pH 4.0		Ammonium hydroxyacetate, pH 4.0	
	BGE/10 (Fig. 5a)	BGE/100 (Fig. 5b)	BGE/10 (Fig. 7a)	BGE/200 (Fig. 7b)
Ionic strength (M)	0.12		0.15	
Proteins				
Cytochrome *c*	464 000 (4 200 000)[a]	120 000	861 000 (4 200 000)[a]	329 000
Lysosyme	750 000 (4 700 000)[a]	161 000	550 000 (4 700 000)[a]	390 000
Ribonuclease A	1 290 000 (3 800 000)[a]	226 000	No data (3 800 000)[a]	670 000
α-Chymotrypsinogen A	1 600 000 (3 700 000)[a]	296 000	1 660 000 (3 700 000)[a]	1 040 000

[a] Theoretical $N_{\max}$ (per meter), calculated from: $N = L_d/\delta^2_{diff}$ and $\delta^2_{diff} = 2Dt$ where L_d is the effective length of the capillary, D the diffusion constant (see Table 1 and Section 3.6.) and t the migration time (the width of the starting zone and all types of zone broadenings are assumed to be 0, except that caused by diffusion). Proteins were dissolved in diluted BGE and were applied at a voltage of 1 kV for 16 s. Separation field strength: 360 V cm^{-1}.

(+ or −) as the protein), the protein and the counter ion, respectively. The mobility has a positive sign for a cation and a negative sign for an anion, as has the protein concentration. It should be noted that the asymmetry of the peaks increases with increasing $\Delta\kappa$, but not always (see Section 2.5.1 in Part I [1]). For restrictions in the application of Eq. (8), see Section 3.8 in Part I [1].

To minimize $\Delta\kappa$, the concentration of the protein should be small, the mobility of the co-ion (the positive buffer ion in the experiments herein where the protein is positively charged) should be close to that of the protein, and the mobility (u_R) of the counter ion (the negative buffer ion in our experiments) should be low. The differences between the mobilities of the proteins and the buffer ions ($u_A = u_P$ in Eq. (8) get larger with an increase in the ionic strength of the buffer and thus the zone distortion (Fig. 12 in Ref. [20]) provided that $|u_{prot}| < |u_{buffer}|$.

As expected, not only the conductivity in a protein zone differs from that in the surrounding buffer, but also the pH. Fortunately, in most cases the tailing (fronting) caused by conductivity differences is counteracted by fronting (tailing) caused by pH differences [1,45].

When the conductivity and pH distortions are so large that one boundary of the protein zone is hyper-sharp, i.e. it is perpendicular to the baseline, the zone broadening is determined by the expressions [1]:

$$\Delta X_{\Delta\kappa} = L\frac{\Delta\kappa}{\kappa} \tag{9}$$

and

$$\Delta X_{\Delta pH} = L\frac{\Delta v}{v} \tag{10}$$

Observe that zone distortions originating from conductivity and pH differences cause no or negligible zone broadening except when one of the boundaries is hyper-sharp (Part I [1]).

3.9. Other factors contributing to zone broadening

Many factors affect the width and the variance of a zone in capillary electrophoresis, e.g. the plug length of the applied sample zone ($\sigma^2_{\Delta x_0}$), longitudinal diffusion (σ^2_{diff}), development of Joule heat ($\sigma^2_{J\,rad\,diff}$), adsorption of analytes to the capillary surface (σ^2_{ads}), conductivity ($\sigma^2_{\Delta\kappa}$) and pH differences ($\sigma^2_{\Delta pH}$) between the solute zone and the surrounding buffer, interaction between proteins and buffer ions, other proteins, etc. (σ^2_{int}), capillary coiling (σ^2_{curv}) and sedimentation (σ^2_{sed}) (all of the above factors are described in detail in Part I). Since independent variances are additive, the total variance for zone broadening is given by the following general relationship (variances corresponding to zone broadenings appearing outside the column being ignored):

$$\sigma^2_{tot} = \sigma^2_{\Delta x_0} + \sigma^2_{diff} + \sigma^2_{J\,rad\,diff} + \sigma^2_{ads} + \sigma^2_{int} + \sigma^2_{curv} + \sigma^2_{sed} \tag{11}$$

The variances in conductivity and pH have not been included here since in most experiments they are zero or negligible (see Section 3.2). Notice that the asymmetry of a peak caused by a conductivity difference is often counteracted by a pH difference (see Section 3.8) [46], which explains why hyper-sharp protein peaks (see Eqs. (9) and (10)) seldom appear in the electropherograms.

The experimental total variances were calculated from the plate numbers (Tables 6 and 7) using the relation:

$$\sigma^2_{tot} = \frac{L^2_d}{N} \tag{12}$$

where L_d is the effective length of the capillary. N is obtained from the statistical moments calculated by the computer program. A list of calculated variances contributing to the total zone broadening is given in Tables 6 and 7 for ammonium acetate and ammonium hydroxyacetate as BGE, respectively. The equations presented in Part I were used for these calculations. For both buffers, when the injected sample is dissolved in BGE diluted 10-fold, among the calculated variances the longitudinal diffusion dominates, the curvature effects are significant (1.6–5.6%), and the injection plug contributes with 0.5–13%, Joule heat effects are small corresponding to 0.02–0.5%, and there is a non-negligible rest variance. The rest variance is, however, not caused by adsorption of the proteins onto the capillary wall since in the presence of adsorption the efficiency should decrease with an increase in field strength, but in our experiments it increases (Fig. 4). The rest variance may have its origin in relatively slow interactions between proteins and buffer constituents, as well as in hyper-sharp peaks (see Part I [1]). It is well known from moving boundary experiments that acetate ions react with some proteins, such as ovalbumin [37]. The rest variance increases strongly with the mobility of the proteins (Tables 6 and 7), which is a strong indication that the main reason for its origin is an interaction with the proteins (see also Fig. 6 in Part I [1]). The effects behind the development of hyper-sharp peaks, caused by conductivity and pH differences, cannot be the reason behind such a relationship. The conductivity effect increases with an increasing mobility difference between the protein and the buffer co-ion and would consequently increase in the opposite direction, i.e. the effect is larger for the slowest migrating protein. The ΔpH-effect often is largest for the most rapidly migrating proteins. However, it should be recalled that Δκ- and ΔpH-effects often counteract each other (see Section 2.7 in Part I [1]).

It should be stressed that the boundary between sample zone and running buffer is very sharp following zone sharpening, probably hyper-sharp, which is in agreement with the experimental finding that the width of the starting zone is only 0.04–0.4 mm (Tables 6 and 7). Observe that these values are based on the assumption that diffusion is the predominant cause for zone broadening. When also other types of zone broadening appear, the calculated ΔX_0 values are larger than the experimentally obtained. In this case the plot is not linear and one should only use the plate height for the lower field

Table 6
Experimentally determined total variance (cm^2) and the calculated variances in ammonium acetate, pH 4.0, ionic strength: 0.12 M (Fig. 12a and b)

	N/m	$\sigma^2_{\text{tot exp}}$	$\sigma^2_{\Delta x_0}$	σ^2_{diff}	$\sigma^2_{\text{J rad diff}}$	σ^2_{sed} ***	σ^2_{curv}	$\Delta\sigma^2 = \sigma^2_{\text{tot exp}} - \sum\sigma^2_{\text{calc}}$
Cytochrome *c*	464 000 (*120 000)	8.62×10^{-3} * (33.3×10^{-3})	4.59×10^{-5} *(1.22×10^{-5})	1.31×10^{-3} *(1.29×10^{-3})	3.43×10^{-6} *(4.26×10^{-6})	2.34×10^{-8} *(2.34×10^{-6})	2.16×10^{-4}	7.00×10^{-3} *(31.7×10^{-3})
Zone width (mm)/zone broadening**	–	1.86 *(3.65)	0.23 *(0.12)	0.72 *(0.72)	0.037 *(0.041)	0.0031 *(0.031)	0.29	1.67 *(3.56)
Lysozyme	750 000 *(161 000)	5.33×10^{-3} *(24.8×10^{-3})	8.54×10^{-6} *(9.44×10^{-6})	1.16×10^{-3} *(1.14×10^{-3})	3.90×10^{-6} *(4.84×10^{-6})	2.89×10^{-8} *(2.89×10^{-6})	2.16×10^{-4}	3.90×10^{-3} *(23.54×10^{-3})
Zone width (mm)/zone broadening**	–	1.46 *(3.15)	0.10 *(0.11)	0.68 *(0.68)	0.039 *(0.044)	0.0034 *(0.034)	0.29	1.25 *(3.06)
Ribonuclease A	1 290 000 *(226 000)	3.11×10^{-3} *(17.7×10^{-3})	2.00×10^{-5} *(1.63×10^{-5})	1.45×10^{-3} *(1.43×10^{-3})	3.14×10^{-6} *(3.92×10^{-6})	2.91×10^{-8} *(2.91×10^{-6})	2.16×10^{-4}	1.38×10^{-3} *(15.9×10^{-3})
Zone width (mm)/zone broadening**	–	1.12 *(2.66)	0.14 *(0.14)	0.76 *(0.76)	0.035 *(0.040)	0.0034 *(0.034)	0.29	0.74 *(2.53)
α-Chymotrypsinogen A	1 600 000 *(296 000)	2.50×10^{-3} *(13.5×10^{-3})	3.20×10^{-4} *(1.33×10^{-6})	1.50×10^{-3} *(1.49×10^{-3})	3.04×10^{-6} *(3.75×10^{-6})	3.39×10^{-8} *(3.39×10^{-6})	2.16×10^{-4}	0.42×10^{-3} *(11.7×10^{-3})
Zone width (mm)/zone broadening**	–	1.0 *(2.32)	0.36 *(0.069)	0.77 *(0.77)	0.035 *(0.039)	0.0037 *(0.037)	0.29	0.41 *(2.16)

Samples were dissolved in 10-and *100-fold diluted buffer.
** 2σ, except for $\Delta X_0(\sqrt{12}\sigma)$.
*** The variance for sedimentation in the vertical section of the capillary (t = 5 min).

Table 7
Experimentally determined total variance (cm^2) and the calculated variances in ammonium hydroxyacetate, pH 4.0, ionic strength: 0.15 M (Fig. 6a and b)

	N/m	$\sigma^2_{\text{tot exp}}$	$\sigma^2_{\Delta x_0}$	σ^2_{diff}	$\sigma^2_{\text{J rad diff}}$	σ^2_{sed} ***	σ^2_{curv}	$\Delta\sigma^2 = \sigma^2_{\text{tot exp}} - \sum\sigma^2_{\text{calc}}$
Cytochrome *c*	861 000 *(329 000)	4.65×10^{-3} *(12.2×10^{-3})	*(1.43×10^{-6})	1.26×10^{-3} *(1.25×10^{-3})	8.21×10^{-6} *(8.14×10^{-6})	3.34×10^{-8} *(9.39×10^{-6})	2.16×10^{-4}	3.12×10^{-3} *(10.7×10^{-3})
Zone width (mm)/zone broadening**	–	1.36 *(2.21)	*(0.04)	0.71 *(0.71)	0.057 *(0.057)	0.0037 *(0.061)	0.29	1.12 *(2.07)
Lysozyme	550 000 *(390 000)	7.27×10^{-3} *(10.3×10^{-3})	*(1.41×10^{-5})	1.13×10^{-3} *(1.12×10^{-3})	9.06×10^{-6} *(8.99×10^{-6})	2.89×10^{-8} *(1.15×10^{-5})	2.16×10^{-4}	5.87×10^{-3} *(8.88×10^{-3})
Zone width (mm)/zone broadening**	–	1.71 *(2.03)	*(0.13)	0.67 *(0.67)	0.061 *(0.060)	0.0034 *(0.068)	0.29	1.53 *(1.89)
Ribonuclease A	*(670 000)	– *(5.97×10^{-3})	*(1.11×10^{-5})	1.40×10^{-3} *(1.40×10^{-3})	7.27×10^{-6} *(7.27×10^{-6})	2.91×10^{-8} *(1.17×10^{-5})	2.16×10^{-4}	– *(4.27×10^{-3})
Zone width (mm)/zone broadening**	–	– *(1.55)	*(0.12)	0.75 *(0.75)	0.054 *(0.054)	0.0034 *(0.068)	0.29	– *(1.31)
α-Chymotrypsinogen A	1 660 000 (*1 040 000)	2.41×10^{-3} *(3.86×10^{-3})	*(1.11×10^{-5})	1.43×10^{-3} *(1.42×10^{-3})	7.21×10^{-6} *(7.28×10^{-6})	3.39×10^{-8} *(1.36×10^{-5})	2.16×10^{-4}	0.71×10^{-3} *(2.15×10^{-3})
Zone width (mm)/zone broadening**	–	0.98 *(1.24)	*(0.12)	0.76 *(0.75)	0.054 *(0.054)	0.0037 *(0.074)	0.29	0.53 *(0.93)

Samples were dissolved in 10-and *200-fold diluted buffer.
** 2σ, except for $\Delta X_0(\sqrt{12}\sigma)$.
*** The variance for sedimentation in the vertical section of the capillary (t = 5 min).

strengths where the deviation from a straight line is smallest. From the slope of the line ($2D/u$) one can easily calculate the diffusion coefficient. If the value obtained is close to the literature value, diffusion is the largest contribution to the zone broadening, i.e. other types of zone broadening are negligible. When the D-value differs from the literature value other types of zone broadening cannot be neglected, and the true ΔX_0-values are smaller than the calculated ones.

In the separation step, the very narrow enriched sample zone became blurred by diffusion and other zone distortions, with the advancing boundary sharpened and the rear boundary blurred by a conductivity difference since $\Delta\kappa$, calculated by Eq. (8), has a negative value; ΔpH is positive, which means that the advancing boundary of the peak became blurred and the rear boundary sharpened, i.e. the electrodispersion and pH dispersion counteract each other, and, thus, create less peak asymmetry, as expected (Section 2.7 in Part I [1]). The shapes of the peaks in many of the electropherograms do not contradict this qualitative discussion.

The widths of the peaks at 60% of the peak height (2σ) for the ammonium acetate and ammonium hydroxyacetate systems (Tables 6 and 7) demonstrate the contribution of the different zone broadening effects in a complementary and enlightening way, some of them contributing significantly to zone broadening. Observe that the width of the starting zone ($\sigma^2_{\Delta x_0}$) is calculated from the expression $\sqrt{12}\sigma$.

The efficiency (N/m) decreases drastically when the sample is injected in 100–200-fold diluted buffers (Tables 6 and 7). The rest variance is then the dominating contribution (87–95% and 59–88% for ammonium acetate and ammonium hydroxyacetate as the BGE, respectively). This contribution decreases with increasing migration times illustrating that it originates from interactions between the sample and the surrounding BGE zones. Careful studies of peak shapes in related electropherograms (Fig. 12b) showed that at least the first three peaks were hyper-sharp. This means that the net contribution of ΔpH and $\Delta\kappa$ effects will increase the zone-broadening, and it is probable that those parameters together with protein–protein and protein–buffer interactions in the highly concentrated zones are responsible for the significantly larger rest variance when the sample solution is highly diluted. However, the advantage of injecting highly diluted samples is improved detection limits, and the resolution seems still to be adequate for studies on protein purity, see Sections 3.10 and 3.11.

3.10. CLOD

The concentration limits of detection (CLODs) of the proteins were determined at pH 4.0 in ammonium acetate and ammonium hydroxyacetate (ionic strengths 0.12 and 0.15 M, respectively), the buffers giving the highest resolution among those tested in this study. The analytes were introduced by electrokinetic injection in 100- and 200-fold diluted BGE, respectively. Stock solutions of the proteins were diluted in order to determine the CLODs, defined as peak heights three times higher than the background noise. The CLODs were significantly lower for ammonium acetate than for ammonium hydroxyacetate (Table 8), although the efficiencies were considerably higher with ammonium hydroxyacetate as BGE (see Table 5). The reason is probably the lower background in the UV signal at 200 nm for acetate compared to that for hydroxyacetate. This relatively large difference in CLODs need not be valid for other detection techniques, e.g. mass spectrometry. In an attempt to improve the detection limits, the volumes of the proteins introduced were expanded by increasing the hydrodynamic injection times (up to 30 s). The areas and heights of the peaks increased, although at the expense of resolution.

Table 8
Comparison of CLOD values of four basic proteins

	Ammonium acetate, pH 4.0 (Fig. 5b)*	Ammonium hydroxyacetate, pH 4.0 (Fig. 7b)**
Ionic strength (M)	0.12	0.15
Proteins		
Cytochrome *c* (pmol/ml)	8	41
Lysozyme (pmol/ml)	5	18
Ribonuclease A (pmol/ml)	6	19
α-Chymotrypsinogen A (pmol/ml)	4	12

The proteins were dissolved in *100- and **200-fold diluted BGE to the final concentrations and were injected by applying 1 kV for 16 s. Separation field strength: 360 V cm^{-1}.

3.11. Evaluation summary of the background electrolytes

A summary of important parameters, determined in experiments in different background electrolytes is shown in Table 9. Four of the BGEs gave excellent efficiencies; the plate number in some cases exceeding 1 million per meter (Table 5). Triethanolamine-hydroxyacetate provided the highest mean value for the four studied proteins. Upon a 10-fold dilution ammonium acetate and ammonium hydroxyacetate (pH 4.0) have similar efficiencies, whereas the latter buffer gives higher efficiencies at higher dilution, probably reflecting its higher buffering capacity.

Triethanolamine-hydroxyacetate was, along with ammonium acetate, the most efficient medium for the resolution of isomer/impurity peaks, followed by ammonium hydroxyacetate. The resolution seems to be strongly dependent on pH, being high at pH 4 and low at pH 3. The pH was generally chosen close to the pK_a value of the acidic component to obtain a high buffering capacity, the pH 3 of the formate buffer being an exception. The comparison is, therefore, unfair towards this buffer, which may give adequate isomer/impurity peak resolution at pH 4, where the buffering capacity is higher. The triethanolamine-hydroxyacetate buffer has the lowest conductivity ($\kappa = \sum c_j u_j$), since its components are relatively large and the pH is very close to the pK_a of the acid

Table 9
Summary of buffer performance

Buffers	Efficiency	Resolution of isomer/impurity peaks	Buffering capacity	κ (see Table 4)	Protein stability	UV absorbance	R.S.D. (for t_m)
Ammonium acetate, pH 4.0 (ionic strength: 0.12 M)	+ + + +	+ + + + +	+ + +	+ + +	+ + + + +	+ + + +	+ + + + +
Ammonium hydroxyacetate, pH 4.0 (ionic strength: 0.15 M)	+ + + +	+ + + +	+ + + + +	+ + +	+ + + + +	+ + +	+ + + +
Ammonium formate, pH 2.7 (ionic strength: 0.067 M)	–	+	+ +	+ +	–	+ + + +	–
Sodium phosphate, pH 3.0 (ionic strength: 0.10 M)	+ + +	–	+ + + +	+	–	+ + + + +	–
Triethanolamine-malonate, pH 3.0 (ionic strength: 0.10 M)	–	–	+ + + + +	+ + + +	–	+	–
Triethanolamine-hydroxyacetate, pH 4.0 (ionic strength: 0.25 M)	+ + + + +	+ + + + +	+ + + + +	+ + + +	+ + +	+	+ +

(3.8). The proteins were highly stable in three of the buffers used: ammonium acetate, ammonium hydroxyacetate and triethanolamine-hydroxyacetate, but seemed to be very unstable in ammonium formate and triethanolamine-malonate. Those two buffers were used at pH 3, as was the phosphate buffer, which also exhibited poor protein stability. Consequently, the instability seems to depend more on the pH of the buffer than its composition. Most of the buffers have some UV absorbance at the wavelength used, 200 nm, especially those containing triethanolamine, whereas the phosphate buffer is the most transparent at this wavelength. The repeatabilities of the migration times were excellent for ammonium acetate, good for ammonium hydroxyacetate, and reasonable for triethanolamine-hydroxyacetate (Table 2). However, in the experiments with the latter buffer a longer injection time was used, which probably affected the precision. The most favorable conditions for high efficiency and resolution of isomer/impurity peaks were obtained when the sample was added to a BGE at pH 4 diluted 10 times. Electropherograms demonstrating these conditions are shown in Figs. 5a and 7a. The efficiencies in the ammonium acetate buffer ranged from 464 000 to 1 600 000 for the four proteins and in ammonium hydroxyacetate from 550 000 to 1 660 000 (Table 5). The other three buffers, which all were used at pH 3, showed large variations in the migration times. To summarize, two of the buffers showed excellent performance for the protein separations: ammonium acetate and ammonium hydroxyacetate at pH 4. One buffer, the triethanolamine-hydroxyacetate, was excellent regarding most criteria but showed some drawbacks in migration time repeatabilities (Table 2) and UV absorbance (probably, this absorption can be decreased by distillation of the triethanolamine or by treatment with active charcoal). The precision in the migration times may be much better if other injection conditions are used, for instance lower voltage during a longer time. Application of the sample by pressure may also increase the precision.

4. Conclusions

The polyacrylamide coating was very stable at neutral and acidic conditions; washing of the capillary with 2 M HCl increased the repeatability of migration times and peak areas. The separation of the four basic proteins at acidic pH depends strongly on the type of the running buffer and its concentration. Acetic and hydroxyacetic acids titrated with ammonia provided high efficiency and resolution of the model proteins, as well as of isomer/impurity peaks (Figs. 5 and 7). Another buffer, triethanolamine-hydroxyacetate, seemed also to be a promising buffer since it gave high efficiency, as well as excellent resolution of isomer/impurity peaks, but with two drawbacks: the high UV-absorbing cation and the low precision in migration times (Table 2). The reason behind the lower precision in the migration times might be shorter injection time used with this buffer (2 s) and a possible variation in current caused by bubbles and/or precipitates (see Section 2.10.3 in Part I [1]).

The other buffer types tested herein (such as ammonium formate, sodium phosphate, triethanolamine-malonate) gave less good repeatability and resolution; furthermore, at pH $\leq$ 3, they probably caused precipitation and/or denaturation of the proteins. Among the tested ionic strengths of the two buffers of choice, ammonium acetate and ammonium hydroxyacetate, 0.12 and 0.15 M were the preferred, respectively. Efficient zone sharpening was achieved with dilution factors as high as 100–200, improving the sensitivity and giving limits of detection at 200 nm in the order of 4–8 pmol/ml of proteins for ammonium acetate and 12–41 pmol/ml for ammonium hydroxyacetate, although a 10-fold dilution of the running buffer gave the highest plate numbers. Sedimentation at the inlet may give rise to loss of protein, as can the washing of the inlet of the capillary. Moderate conductivity and pH differences cause zone distortions, but no or negligible zone broadening at low dilution degree of the sample solution.

However, at high dilutions of the sample hyper-sharp peaks were obtained for which conductivity and/or pH effects cause significant zone-broadening. The same is true for interactions between a protein and a buffer constituent, other proteins, capillary coating, etc., provided that the on/off kinetics is slow enough (Part I [1]). There are, accordingly, reasons why different buffers give different plate numbers. The rest variances calculated for ammonium acetate and ammonium hydroxyacetate increases strongly with increasing mobility of the proteins, indication of the presence of interaction between the proteins and the buffer components. A closer study on the theoretical aspects on some of the data obtained experimentally is given in Part I of this series [1].

Acknowledgements

This investigation has been supported economically by The Swedish Research Council and The Carl Trygger Foundation.

References

[1] S. Hjertén, S. Mohabbati, D. Westerlund, J. Chromatogr. A 1053 (2004) 181.
[2] M.C. Millot, C. Vidal-Madjar, P.R. Brown, E. Grushka, Adv. Chromatogr. 40 (2000) 427;
K.A. Denton, R.J. Harris, J. Chromatogr. A 705 (1995) 335.
[3] E. Jäverfalk-Hoyes, U. Bondesson, D. Westerlund, P. Andrén, Electrophoresis 20 (1999) 1527.
[4] Y. Shen, R. Smith, Electrophoresis 23 (2002) 3106.
[5] V. Dolnik, K.M. Hutterer, Electrophoresis 22 (2001) 4163.
[6] J. Patrick, A. Lagu, Electrophoresis 22 (2001) 4179.
[7] P.G. Righetti, Biopharm. Drug Dispos. 22 (2001) 337.
[8] M. Chiari, M. Nesi, P.G. Righetti, Capillary Electrophoresis in Analytical Biotechnology, CRC Press, Boca Raton, FL, 1996, pp. 1–36.
[9] S. Hjertén, K. Kubo, Electrophoresis 14 (1993) 390.
[10] S. Hjertén, Chromatogr. Rev. 9 (1967) 122.
[11] S. Hjertén, Ark. Kemi. 13 (1958) 151.
[12] D.J. Corradini, J. Chromatogr. B 699 (1997) 221.
[13] D. Tietz, M.H. Gottlieb, J.S. Fawcett, A. Chrambach, Electrophoresis 7 (1986) 217.
[14] S. Hjertén, J. Chromatogr. 347 (1985) 191.
[15] K.A. Cobb, V. Dolnik, M. Novotny, Anal. Chem. 62 (1990) 2478.
[16] M. Chiari, M. Nesi, J.E. Sandoval, J.J. Pesek, J. Chromatogr. A 717 (1995) 1.
[17] C. Gelfi, M. Curcio, P.G. Righetti, R. Sebastiano, A. Citterio, H. Ahmadzadeh, N.J. Dovichi, Electrophoresis 19 (1998) 1677.
[18] H. Wan, M. Öhman, L.G. Blomberg, J. Chromatogr. A 924 (2001) 59.
[19] D. Belder, A. Deege, H. Husmann, F. Kohler, M. Ludwig, Electrophoresis 22 (2001) 3813.
[20] L. Ornstein, Disc Electrophor. 121 (1964) 321.
[21] S. Hjertén, Electrophoresis 2 (1990) 665.
[22] F. Foret, E. Szökő, B.L. Karger, Electrophoresis 14 (1993) 417.
[23] S. Hjertén, J.-L. Liao, R.J. Zhang, J. Chromatogr. A 676 (1994) 409.
[24] S. Liao, R. Zhang, S. Hjertén, J. Chromatogr. A 676 (1994) 421.
[25] Q. Mao, J. Pawliszyn, W. Thormann, Anal. Chem. 72 (2000) 5493.
[26] J. Cann, Electrophoresis 19 (1998) 1577.
[27] S. Hjertén, Biochim. Biophys. Acta 32 (1959) 531.
[28] Z.K. Shihabi, M. Friedberg, J. Chromatogr. A 807 (1998) 129.
[29] R. Zhang, S. Hjertén, Anal. Chem. 69 (1997) 1585.
[30] H. Haglund, A. Tiselius, Acta Chem. Scand. 4 (1950) 957.
[31] S. Hjertén, S. Jerstedt, A. Tiselius, Anal. Biochem. 11 (1965) 219.
[32] Y. Liu, R. Fu, J. Gu, J. Chromatogr. A 694 (1995) 498.
[33] J.A. Lux, U. Hausig, G. Schomburg, J. High Resolut. Chromatogr. 13 (1990) 373.
[34] L.G. Öfverstedt, G. Johansson, G. Fröman, S. Hjertén, Electrophoresis 21 (1981) 168.
[35] M.D. Zhu, J.C. Chen, S. Hjertén, US Pat. 5089111; filed 27 January 1989 and 27 September 1990, Approved February 1992.
[36] D.N. Heiger, A.S. Cohen, B.L. Karger, J. Chromatogr. 516 (1990) 33.
[37] M. Bier, Electrophoresis, Academic Press, New York, 1959, p. 101.
[38] D. Corradini, A. Rhomberg, C. Corradini, J. Chromatogr. A 661 (1994) 305.
[39] D. Corradini, G. Cannarsa, E. Fabbri, C. Corradini, J. Chromatogr. A 709 (1995) 127.
[40] B. Verzola, C. Gelfi, P.G. Righetti, J. Chromatogr. A 868 (2000) 85.
[41] F. Foret, L. Křivánková, P. Boček, Capillary Zone Electrophoresis, VCH, New York, 1993, pp. 38–40.
[42] H.C. Cox, J.K.C. Hessels, J.M.G. Teven, J. Chromatogr. 66 (1972) 19.
[43] J.W. Williams, K.E. van Holde, R.L. Baldwin, Chem. Rev. 58 (1958) 715.
[44] C.J.O.R. Morris, P. Morris, Separation Methods in Biochemistry, Pitman, London, 1976, pp. 705–760.
[45] S. Hjertén, in: G. Milazzo (Ed.), Topics in Bioelectrochemistry and Bioenergetics, vol. 2, Wiley, 1978, pp. 89–128.
[46] X. Xu, W.Th. Kok, H. Poppe, J. Chromatogr. A 742 (1996) 211.